

Faraday Discussions

Accepted Manuscript



This manuscript will be presented and discussed at a forthcoming Faraday Discussion meeting. All delegates can contribute to the discussion which will be included in the final volume.

Register now to attend! Full details of all upcoming meetings: <http://rsc.li/fd-upcoming-meetings>



This is an *Accepted Manuscript*, which has been through the Royal Society of Chemistry peer review process and has been accepted for publication.

Accepted Manuscripts are published online shortly after acceptance, before technical editing, formatting and proof reading. Using this free service, authors can make their results available to the community, in citable form, before we publish the edited article. We will replace this *Accepted Manuscript* with the edited and formatted *Advance Article* as soon as it is available.

You can find more information about *Accepted Manuscripts* in the [Information for Authors](#).

Please note that technical editing may introduce minor changes to the text and/or graphics, which may alter content. The journal's standard [Terms & Conditions](#) and the [Ethical guidelines](#) still apply. In no event shall the Royal Society of Chemistry be held responsible for any errors or omissions in this *Accepted Manuscript* or any consequences arising from the use of any information it contains.



Journal Name

ARTICLE

Mechanical matching between ligand and receptor

A. Peñaherrera^a

Received 00th January 20xx,
Accepted 00th January 20xx

DOI: 10.1039/x0xx00000x

www.rsc.org/

Interactions between ligands and receptors and subsequent “locking” must involve some resistance to unbinding manifesting itself as an interaction force^{6,8}. At body temperature, spontaneous unbinding will occur however external forces are required to accelerate this process. Bearing in mind the potential forces that the receptor ligand complex is likely to be subjected to in a biological environment, it might be hypothesised that there is some mechanical matching between receptor and ligand. To test this hypothesis various receptor and ligands were unfolded in their entirety in order to determine their total unfolding force. In this manner the total force to unfold the protein could be determined allowing a comparison between ligand and receptor pairs. The interest of this work is to examine the interaction between five proteins and mica surface by AFM without any modification to preserve nature elastic properties of protein molecules during force measurements. The results showed a mechanical matching between GP120 (ligand) and CD4 (receptor) when analysing the total force required to unfold the same number of domains or events shown by the force distance curves of these proteins.

Introduction

The first time AFM was used to mechanically unfold proteins was when the giant protein titin found in muscle was spanned between the AFM tip and the support. Separating these two from each other led to the unfolding of the titin domains and the corresponding forces were measured with the Bell's theory described by Evans and Ritchie in 1997^{1,2}. Mechanical experiments performed on single biomolecules offer invaluable insights into their structure and function³. Importantly, the unfolding force could not be considered naively as a fixed characteristic value, due to dynamic force spectroscopy, varying the pulling rate, demonstrated as the pulling rate increases, the unfolding force measured becomes higher^{2,4,5}. Whereas the vertical tip jump during pull-off makes it possible to estimate the interaction forces, the width and shape of the retraction curve are indicative of molecular elongation processes associated with entropically unfavourable molecular unfolding and elongation⁶. AFM has been successfully utilized to measure intramolecular unfolding forces of individual proteins and intermolecular forces between various ligands and receptor pairs. Remarkably, the force needed to separate a ligand from its specific binding site is different from the force required to remove a non-

specifically bound ligand^{6,8}.

The elastic properties of stretching proteins can be described with the worm-like chain (WLC) model for entropic elasticity. Equation 1 describes the approximate analytic formula³.

This model dictates that the force needed to stretch a linear polymer in a solvent to a length x is given by Bustamante, *et al.* (1994) in which b is the persistence length and L is the contour length^{9,10}.

$$F(x) = \left(\frac{kT}{b}\right) \left[0.25 \left(1 - \frac{x}{L}\right)^{-2} - 0.25 + \frac{x}{L}\right] \text{Equation 1}$$

When the adsorption properties of free floating molecules are desired, force spectroscopy of surface bound proteins with a naked tip can elucidate wealth of information¹¹. However, the surface reactivity of Fn depends on how Fn exhibits its binding sites when adsorbed on a surface¹². Moreover, several surface properties have been proposed to influence protein adsorption and cell behaviour, for instance: charge, topography, surface energy and surface chemistry¹³.

Many proteins with mechanical functions such as the muscle protein titin, extracellular matrix (ECM) proteins fibronectin and tenascin as well as other proteins that participate in cellular adhesion like cadherins, are composed of similarly structured globular domains connected series. Commonly, they consist of a

^a Department of Chemical Engineering and Advanced Materials, Newcastle University, Newcastle Upon Tyne, NE1 7RU, UK

ARTICLE

single polypeptide chain that is able to locally fold into well-separated domains. These domains act like beads on a string and this design favours the entropic elasticity of the protein that can be then exploited in modulating the length and tension of various proteinaceous elastic cellular structures¹⁴.

Cellular adhesion is mainly mediated by integrins, cell-surface receptors that comprise an expanding family of transmembrane heterodimers of a α and β subunit. Integrins have been considered to play a key role in the malignant behaviour of neoplastic cells. Integrins recognize fibronectin through the RGD site that is comprised in the 10th type III repeat (10FNIII). Integrin binding to Fn RGD-loop on 10FNIII results in the formation of a cytoskeletal apparatus that mechanically joins actin contractility to extracellular fibronectin fibers¹⁵.

Protein assembly at interfaces is essential to disease pathology and biological function. HIV-1 envelope glycoprotein mediates the fusion of viral and target cell membranes, the first critical step anticipating infection¹⁶. The precursor of the envelop protein, GP160, constitutes a trimer and is then sliced by a furin-like protease into two noncovalently connected fragments GP120 for receptor binding and GP41 for membrane fusion¹⁷ as schematically depicted in Figure 1.

The self-assembly of the HIV envelop protein GP160 and its interaction with lipid bilayers have been studied¹⁸. Two ways of assembly were seen, pore and large aggregates formation. They also observed that GP160 sank in one component lipid bilayer over time. Activation of GP160 demands cleavage into two fragments, GP41 which is the transmembrane section and GP120 the protruding spike¹⁸. Spikes of Gp120 protruding from the viral envelope bilayer interact with CD4 and co-receptors embedded in the target cell membrane, anchoring the virion to the cell¹⁹ as illustrated in Figure 2.

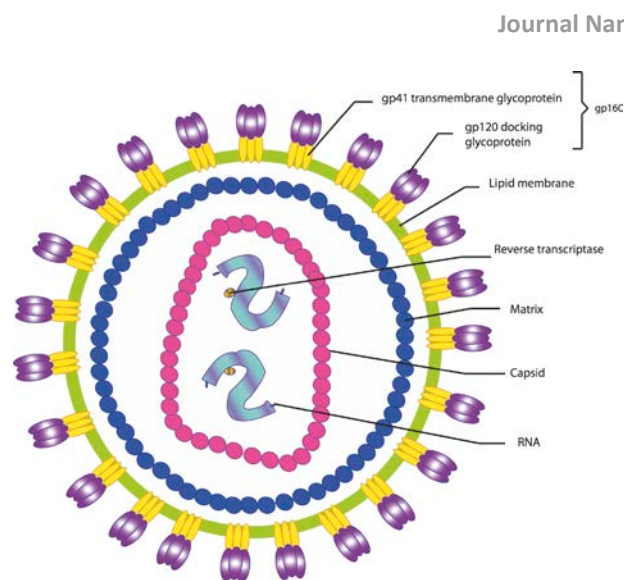


Figure 1 Schematic diagram of Human Immunodeficiency Virion. A lipid bilayer delivered from the host contains the viral glycoproteins GP41 and GP120, which together form GP160.

Table 1 Receptor-ligand pairs

Receptor	Ligand
CD4	GP120
Integrin	Fibronectin

CD4 belongs to Type I membrane proteins that consist in four extracellular immunoglobulin-like domains, a transmembrane fragment and a cytoplasmic tail. It is present on cell surfaces of T lymphocytes, monocytes, macrophages, dendritic cells, and brain microglia, which are the main target cells for primate immunodeficiency viruses *in vivo*¹⁹.

AFM is suitable to measure the self-assembly properties of proteins and their interaction with lipids. Furthermore, AFM offers molecular level lateral resolution and subnanometer vertical resolution in a liquid environment. In force spectroscopy mode, AFM can unfold proteins of interest at defined locations that facilitates nanomechanical identification of system components¹⁸.

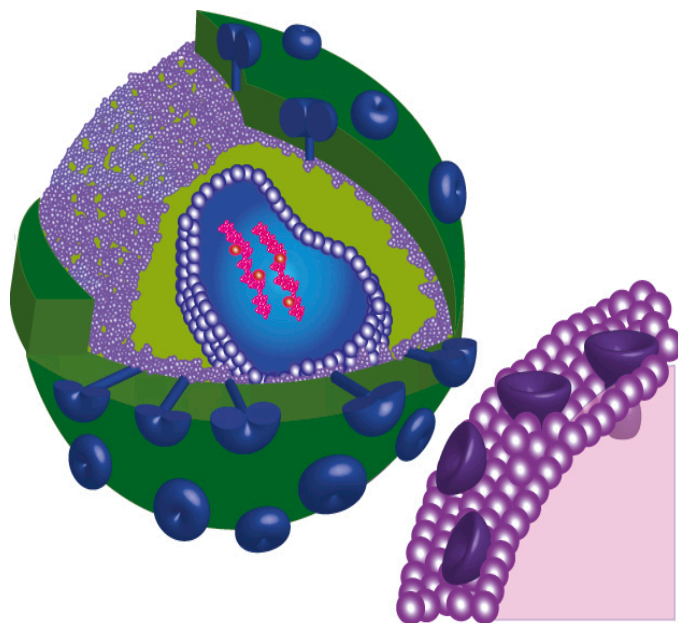


Figure 2 Schematic illustration of GP120 spikes (blue) protruding from the viral envelope bilayer that interact with CD4 (purple).

Complications associated with ensuring proper molecular orientation, conformation and careful control over the instrument mandate careful interpretation of the force data⁵. In this fashion, there is a new way to consider protein domains, which may be interacting with the surface. Researches suggest that by analysis of all peaks in the fibronectin unfolding pattern, a parameter they refer to as total unfolding force, any fibronectin domains which are interacting with the surface are considered within the total unfolding force, in spite of the exact nature of each individual interaction is unknown¹⁸.

Interpreting sawtooth patterns relating to unfolding of protein from a surface is challenging. To this end, a number of factors need to be taken into consideration. Firstly, the conformation of the protein may vary between according to the surface. Secondly, there is not manner to anticipate in which orientation the tip will pick up the protein and whether it adsorbs to the tip via a single or multiple interactions. Finally, identifying which peak(s) in the sawtooth pattern relate to protein-surface interactions is extremely difficult, and these may vary according to the characteristics of the underlying surface¹⁸.

Many reports of AFM studies have measured the force required to separate the ligand from the receptor. For instance, streptavidin-biotin system with average rupture forces indicated between 200 to 409 pN^{20,21}. Moreover, Hussain *et al.* (2005) examined the interactions between Integrin $\alpha_{IIb}\beta_3$ and fibrinogen. However, the present work examines the interaction between various partners of ligand and receptor molecules and mica surface. By employing the strategy suggested by Donlon, *et al* (2012) and therefore, analysing all the peaks in the sawtooth pattern exhibited by each molecule. A mechanical matching has been observed between ligand and receptor when comparing like to like force distance curves. It means that curves that show the same amount of events were compared for each ligand-receptor partner.

Results and discussion

Fibronectin total force measurement

By analysing all peaks in the fibronectin unfolding pattern, a parameter referred as total unfolding force¹⁸, domains which may be interacting with mica are considered. This analysis provides a valuable means to contrast ligand/receptor behaviour on the same surface. The mean total unfolding force for fibronectin is 589.13 ± 64.58 pN as it can be appreciated in Figure 3a.

Donlon, *et al.* 2012 suggested a compact conformation of fibronectin on mica. This conformation would minimize protein-surface interactions; therefore the total unfolding force would decrease. As shown in Figure 3b, a distribution between three to ten events is observed. It is possible to compare like with like curves containing the same number of events¹⁸ that may suggest similar protein conformations between fibronectin (ligand) and integrin (receptor).

As schematically depicted in Figure 4, fibronectin is a multidomain protein where each domain can be classified into one of three distinct types (I, II, or III). The 10th III repeat (10FNIII) comprises the RGD site that is required for integrin recognition. This repeat has been suggested to unfold as a result of cell-traction forces and this unfolding makes possible fibrillogenesis²³. As such, 10FNIII has become a model to understand the unfolding pathway of Fn-III modules¹⁵. One of the most significant contributions of AFM is that Fn-III modules vary significantly in mechanical stability, suggestion the order of Fn-III unravelling is important to its function^{14,21}.

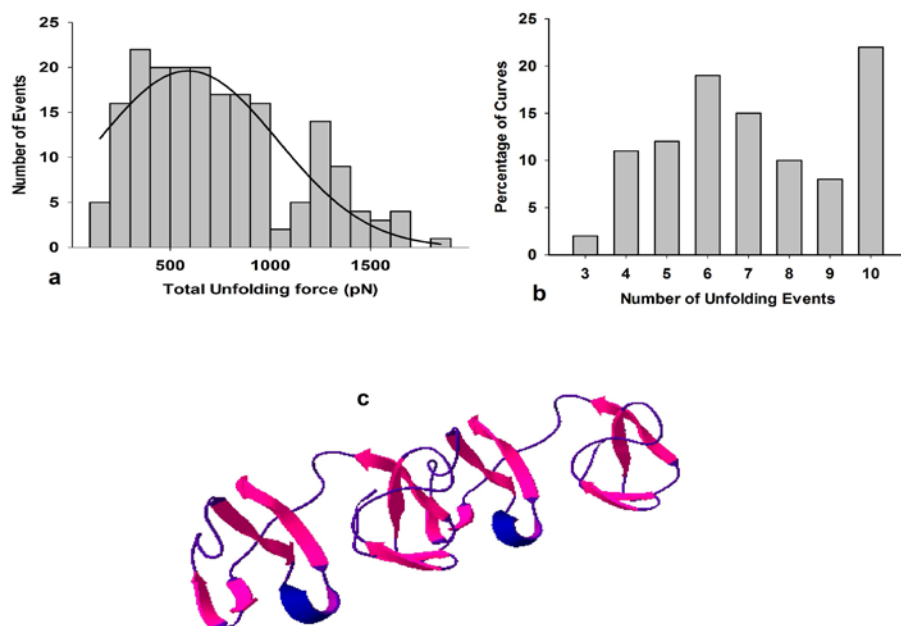


Figure 3 Histogram of total unfolding force distribution of fibronectin on mica. The average of total unfolding force distribution is $589.13 \text{ pN} \pm 64.58$ (Mean= 589.13, SD= 64.68, N=195) (a) Distribution of the number of unfolding events in the sawtooth patterns for the force unfolding of fibronectin on mica. An unfolding event is recognized by a peak in the sawtooth pattern of the force distance curve. Final detachment of the protein from the tip (the last peak in the sawtooth pattern is included in the count). The percentage of curves showing a given number of unfolding events are indicated. Only curves which could be fitted to the worm-like chain model were considered. (b) PDB image of fibronectin (Protein Data Bank). Two fibronectin monomers join through disulphide bonds. β -strands from the upper and lower β -sheet are shown (c)

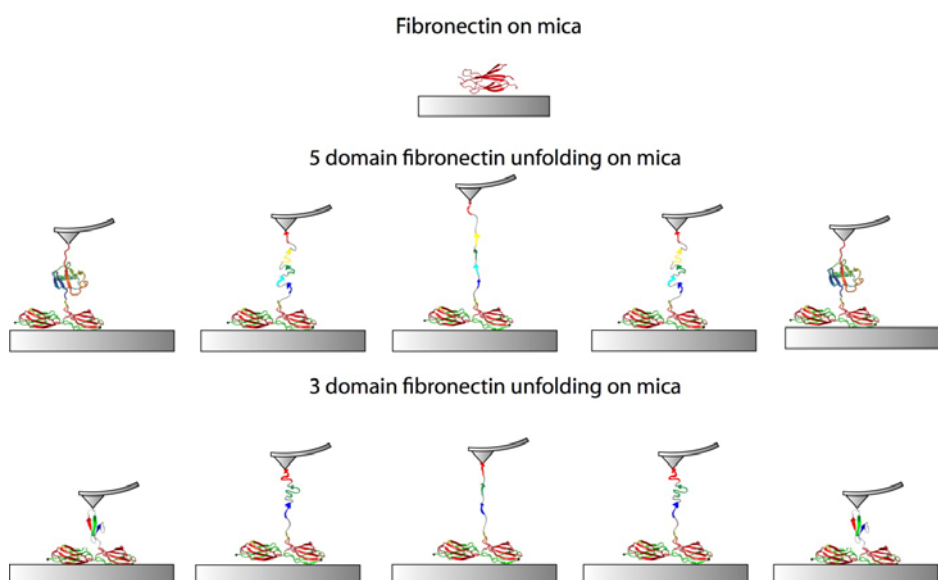


Figure 4 Schematic representations of five and three domains of fibronectin being unfolded.

10FNIII module was determined to be mechanically one of the weakest Fn-III modules and that β -strands progress from a twisted to an aligned state prior to unravelling²⁴. Gao, *et al.* used multiple unfolding simulations of 10FNIII solvated in a water box to stretch it into its completely unfolded form. It is worth mentioning that all $-\beta$ domains from proteins of muscle or the extracellular matrix resist significantly β higher forces than all $-\alpha$, or mixed α/β proteins even where they may be expected to experience stress *in vivo*²⁴. In this report, fibronectin force distance curves exhibited 10 events, which relates to 10 domains and the total force needed to unfold a certain number of domains was compared to its corresponded receptor, integrin.

Integrin total force measurement

The mica surface is atomically flat over large terrace areas thus it is excellent for high resolution imaging of single molecules. Nordin, *et al.* 201 observed integrin aggregates on mica surface, which may be necessary to stabilise the transmembrane protein because of the weak interaction with mica⁸. The mean total unfolding force identified for integrin is 183.99 ± 21.36 pN (Figure 5) which is lower than total unfolding force determined for fibronectin. Besides, force distance curves of the adsorbed integrin exhibit unfolding events, as well as detachment of the integrin from the tip. This result is consistent with weak integrin-mica interactions observed by Nordin, *et al.* 2011.

Force distant curves of integrin on mica exhibit between two and ten events, which makes possible to compare ligand-receptor total unfolding force according to each number of events (figure 5b).

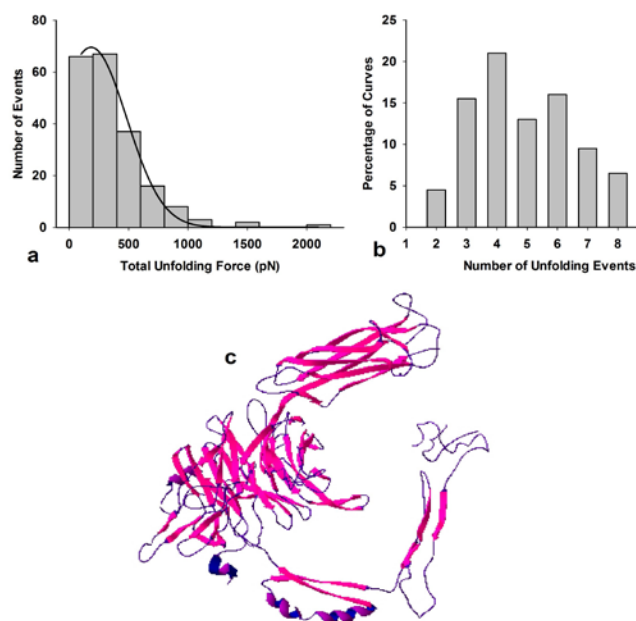


Figure 5 Histogram of total unfolding force distribution of integrin on mica. The average of total unfolding force distribution is 183.99 pN ± 21.36 (Mean= 183.99 , SD= 21.36 , N= 200) (a), Distribution of the number of unfolding events in the sawtooth patterns for the force unfolding of integrin on mica (b) PDB image of integrin (Protein Data Bank) (c).

CD4 total force measurement

A histogram of total unfolding force of CD4 on mica can be appreciated in figure 6. It describes an average value of 655.38 ± 33.17 pN.

GP120 total force measurement

Force distance curves of GP120 on mica revealed well defined sawtooth patterns in the retraction curve, which are characteristic of protein unfolding with individual peaks corresponding to the unfolding of individual protein domains¹⁸.

A histogram of total unfolding force of GP120 on mica indicates an average value of 324.99 ± 35.52 pN (figure 7a).

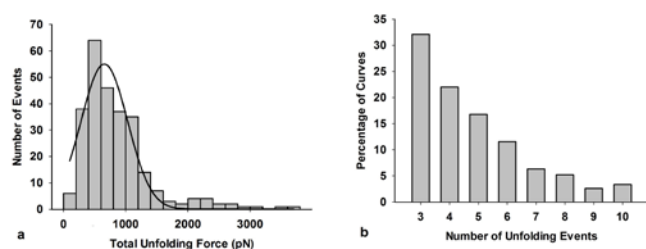


Figure 6 Histogram of total unfolding force distribution of CD4 on mica. The average of total unfolding force distribution is $655.37 \text{ pN} \pm 33.17$ (Mean=655.37, SD= 33.17, N=268) (a) Distribution of the number of unfolding events in the sawtooth patterns for the force unfolding of CD4 on mica (b) PDB image of CD4 (Protein Data Bank) (c).

GP160 total force measurement

Unfolding of single GP160 molecules on mica reveals characteristic, well defined sawtooth patterns in the retraction curve, which is an indicative of protein unfolding with individual segments corresponding to the unfolding of single protein domains. Unfolding forces were extracted by fitting the peaks in the sawtooth pattern to the worm like chain model. The final peak in the sawtooth pattern was discarded due to the fact that it corresponds to detachment of the protein from the tip rather than the protein from the surface, therefore it relates to the interaction between silicon nitride and GP160¹⁸.

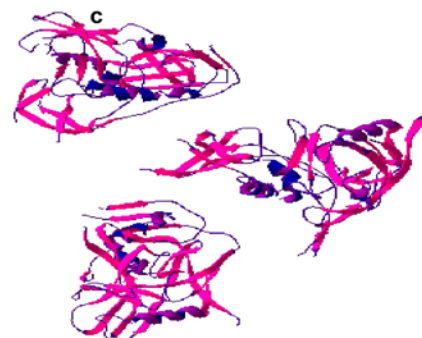
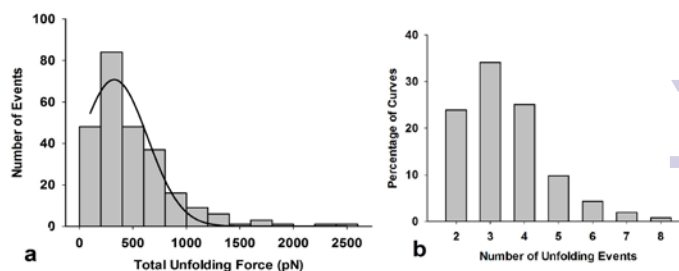


Figure 7 Histogram of total unfolding force distribution of GP120 on mica. The average of total unfolding force distribution is $324.99 \text{ pN} \pm 35.52$ (Mean=324.99, SD= 35.52, N=255) (a), Distribution of the number of unfolding events in the sawtooth patterns for the force unfolding of GP120 on mica (b) PDB image of GP120 (Protein Data Bank) (c).

A histogram of total unfolding force of GP160 on mica can be observed in figure 9a. It shows an average value of $289.47 \pm 11.07 \text{ pN}$. It is worthwhile to note that Donlon and Frankel. (2012) found out that GP160 is considerably easier to unfold when aggregated than isolated.

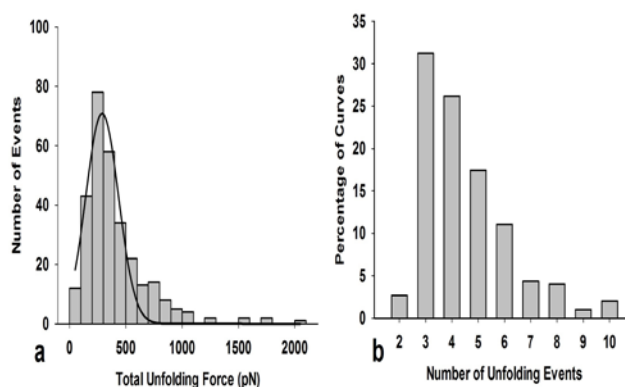


Figure 8 Histogram of total unfolding force distribution of GP160 on mica. The average of total unfolding force distribution is $289.47 \text{ pN} \pm 11.07$ (Mean=239.47, SD= 11.07, N=298) (a) Distribution of the

number of unfolding events in the sawtooth patterns for the force unfolding of GP160 on mica (b).

Total force required to unfold each protein

For this study, the total unfolding forces of ligand and its respective receptor were compared to look at their mechanical properties and try to elucidate mechanical relationship. For instance, total force to unfold three domains of fibronectin was contrasted to total force to unfold three domains of integrin. The purpose is to compare mean total force with all unfolding events because different proteins have different distribution of unfolding events as it can be observed in figure 10.

Results are presented as mean \pm standard error. Statistical analysis was carried out using a Student's *t* test and 2 tailed ANOVA between each ligand and receptor pair according to the number of events.

In the case of GP120 and CD4 a mechanical matching was revealed due to the fact that *p* values were higher than α ($\alpha = 0.05$) in each comparison (3-7 events). Therefore, there is not significant difference between the total force required to unfold the same number of domains of GP120 and CD4. In contrast, GP160 and CD4 do not show mechanical matching ($p < \alpha$) in any comparison as expected due to CD4 binds GP120 and not GP160.

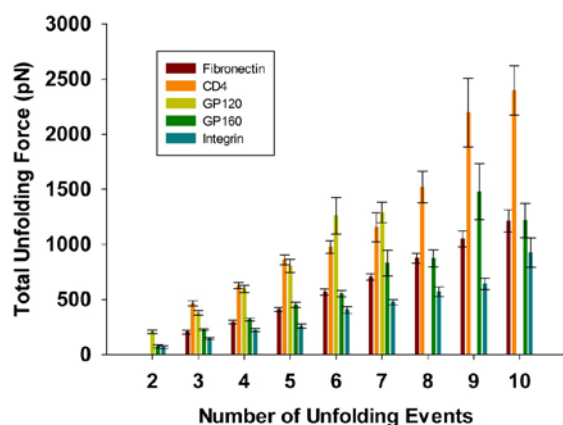


Figure 9 Total force required to unfold each protein according to the number of events. All force distance curves displaying at least two unfolding events as well as detachment of the protein from the tip were considered.

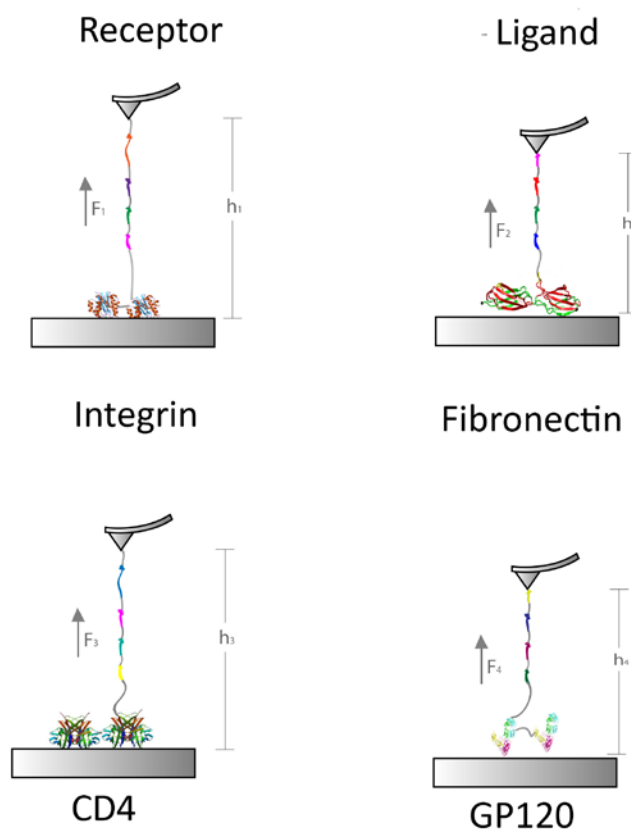


Figure 10 Schematic representation of ligand/receptor mechanical matching. Fn and integrin showed a mechanical matching when 10 domains are unfolded, while GP120 and CD4 showed it in all comparisons (3-7 domains).

Fn and integrin total force values showed *p* values lower than α in almost all comparisons. Except when comparing 10 events total unfolding force because the *p* value obtained for this test was $p = 0.11$. Then, there is not significant difference in total force when 10 Fn and integrin domains are unfolded.

As illustrated by figure 10, the force required to unfold the same number of domains between ligand and receptor is compared.

Experimental

Fibronectin adsorption

Fibronectin from bovine plasma Sigma-Aldrich, UK was dissolved in phosphate buffered saline (PBS) (NaCl 0.138 M; KCl 0.0027 M; Na₂HPO₄·2H₂O 0.01 M; KH₂PO₄ 0.002 M with pH 7.4 at 25°C) to

acquire a concentration of 50 $\mu\text{g/ml}$ protein stock solution. Fibronectin was placed onto mica for 30 minutes (20 x20 mm).

Integrin adsorption

Integrins used in this study were extracted from the Chinese Hamster Ovary cell line, CHO, derived as a Recombinant Human Integrin, $\alpha 5\beta 1$ also known as VLA5 (R&D Systems, Inc., Minneapolis, MN 55413 USA). Integrin was lyophilized from a 0.2 μm filtered solution in TrisCitrate and NaCl. Subsequently the protein was reconstituted in sterile PBS to make 100 $\mu\text{g/mL}$ stock solutions and stored at $-20\text{ }^\circ\text{C}$. Integrin with a concentration of 1 $\mu\text{g/mL}$ was used for adsorption onto freshly cleaved mica surface, and left for a period of between 10 to 30 minutes.

HIV GP120 and CD4 adsorption

Aliquots of HIV GP120 (ab69717, Abcam, UK) and CD4 (ab39483, Abcam, UK) were diluted in ultrapure water to a working concentration of 20 $\mu\text{g/ml}$. Aliquots of stock solution were stored at $-20\text{ }^\circ\text{C}$ with further dilutions were carried out as necessary in ultrapure water. Proteins were adsorbed on mica surface (20 x 20 mm) for 30 minutes within the AFM liquid cell. Prior to imaging surfaces were gently washed 3 times with ultrapure water to remove residual, non-adsorbed protein.

HIV GP160 adsorption

Aliquots of HIVGP160 (ab73770, Abcam, UK) were diluted in ultrapure water to a final concentration of 20 $\mu\text{g/ml}$; aliquots of stock solution were stored at $-20\text{ }^\circ\text{C}$. Further dilutions were carried out as necessary in ultrapure water. Protein was adsorbed for 30 minutes onto mica within the AFM liquid cell. Surfaces were then gently washed 3 times with ultrapure water to remove non-adsorbed protein prior to imaging.

Topographic AFM imaging

AFM experiments were conducted on an Agilent 5500 AFM/SPM microscope in a liquid environment (ultrapure water) at $20\text{ }^\circ\text{C}$.

Images were obtained in contact mode utilizing standard nitrogen doped silicon tips with a nominal force constant of $0.02\text{--}0.77\text{ N m}^{-1}$. Forces were minimized during the scans. Typical scan rates were in the range of 0.5–1 kHz at 512-pixel resolution. Imaging forces were kept below 1 nN.

Force spectroscopy. Force spectroscopy experiments are illustrated in Figure 11 and they were performed using backside aluminium coated silicon cantilevers (PPP-CONTR, Nanosensors, Switzerland) with a nominal spring constant of $0.02\text{--}0.77\text{ N m}^{-1}$ and typical tip radius of less than 7 nm. Spring constants were calibrated using the equipartition theorem (Thermal K) as described by Hutter and Bechhoefer (1993) 1000 force distance curves were obtained per sample with an applied load in the range of 9–10 nN, tip velocities between 0.1 and 10 $\mu\text{m s}^{-1}$ and curve length of 1 μm . Force distance curves were analysed using Scanning Probe Image Processor (SPIP) software version 5.1.6 (Image Metrology, Lyngby, Denmark). Only force curves that fitted to the wormlike chain model were accepted to represent single molecule pulling events, from which unfolding forces were obtained. Determination of rupture forces and loading rates from force-distance spectra was carried out according to previously reported procedures (Faull *et al.*, 1993; Slade *et al.*, 2002).

Force spectra were taken on bare mica before and after protein unfolding on each surface to rule out tip contamination. Drift was minimised by allowing the tip to equilibrate in the liquid cell prior to unfolding measurements. Images before and after spectra showed insignificant drift within the time frame of experiments.

Force spectra were taken on bare mica before and after protein unfolding to rule out tip contamination. Drift was minimised by allowing the tip to equilibrate in the liquid cell prior to unfolding measurements. Images before and after spectra showed insignificant drift within the time frame of experiments.

Journal Name

ARTICLE

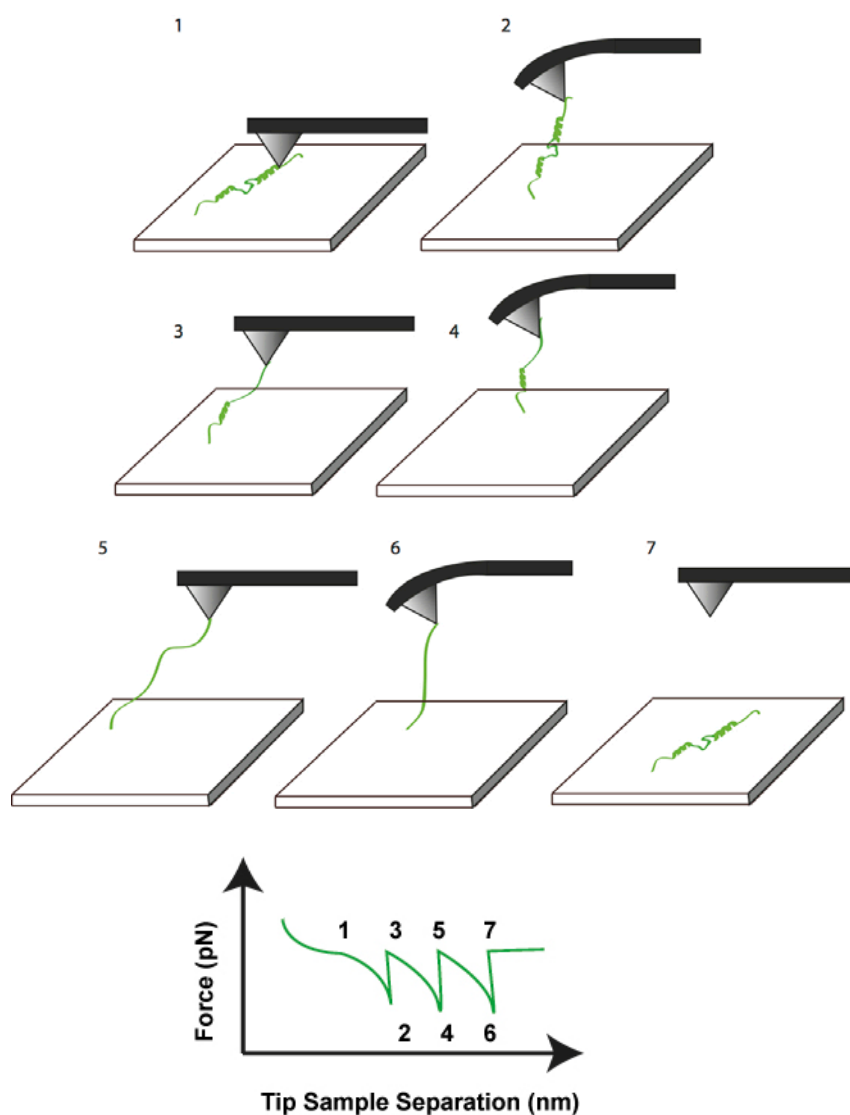


Figure 11. Representation of two domains of protein unfolding on mica surface (top) with a sawtooth pattern on the retraction curve that exemplifies the unfolding events and the subsequent detachment of the tip from the protein. Protein physisorbs to the tip (1) and becomes elongated as the tip retracts. When enough adhesion exists between the tip and the protein, domain denaturation events occur, corresponding to the rupture of more stable domains (2 and 4, respectively). Upon a critical elongation, the protein detaches from the tip, returns to its original conformation and remains on the surface (6-7).



Journal Name

ARTICLE

Conclusions

Mechanical matching between GP120 (ligand) and CD4 (receptor) has been demonstrated when comparing the same number of events unfolding total force. It is possible to compare like with like which may suggest similar protein conformations and unfolding behaviour. These results provide a framework for understanding the complex entry of HIV into cells and should guide efforts to intervene.

The nature elastic properties of protein molecules were maintained during force measurements because there was not AFM tip or substrate modification. This approach allows to relate these findings to real biological systems due to the dependence of protein conformation and thus unfolding force upon the underlying surface characteristics, mainly features like surface chemistry and topography focus the attention to the importance of measuring interactions under condition which mimic those found *in vivo* as accurately as possible.

However, there is no way to know in which orientation the tip will pick up the protein and if it adsorbs to the tip through single or multiple interactions. Multiple orientation and attachment sites within the protein are possible although these may average out whether enough curves are considered.

The total unfolding force is obtained from summation of all individual unfolding events. The distribution of number of unfolding events varies according to the protein. Fibronectin, integrin and GP160 showed between three to ten events. While GP120 showed from two to seven events. In contrast to CD4, that exhibited from three to ten events.

Acknowledgements

The author is grateful to Dr. Daniel Frankel, Dr. Darman Nordin and Dr. Lynn Donlon for their assistance with the AFM analysis of the force distance curves.

References

- 1 G. Bell, *Science*, 1978, 200, 618.
- 2 E. Evans, and K. Ritchie, *Biophysical Journal*, 1997, 72, 1541.
- 3 D. Makarov, Z. Wang, J. Thompson and H. Hansma, *Journal of Chemical Physics*, 2002, 16, 7760.
- 4 M. Rief, M. Gautel, A. Schemmel and H. Gaub, *Biophysical Journal*, 1998, 75, 3008.
- 5 I. Casuso, F. Rico and S. Scheuring, *Journal of Molecular Recognition*, 2011, 24, 406.
- 6 C. Yip, *Current Opinion in Structural Biology*, 2001, 11, 567.
- 7 C. Lee, Y. Wang, L. Huang and S. Lin, *Micron*, 2007, 38, 446.
- 8 D. Nordin, O. Yarkoni, N. Savinykh, L. Donlon and D. Frankel, *Soft Matter*, 2011, 7, 10666.
- 9 C. Bustamante, J. Marko, E. Siggia and S. Smith, *Science*, 1994, 265, 1599.
- 10 H. Mueller, H. Butt and E. Bamberg, *Biophysical Journal*, 1999, 76, 1072.
- 11 L. Donlon and D. Frankel, *Soft Matter*, 2012, 9, 283.
- 12 J. Hull, G. Tamura and D. Castner, *Biophysical Journal*, 2007, 93, 2852.
- 13 E. Velzenberger, I. Pezron, G. Legeay, M. Nagel and K. Kirat, *Langmuir*, 2008, 24, 11734.
- 14 P. Marszalek and Y. Dufrène, *Chemical Society Reviews*, 2011, 41, 3523.
- 15 M. Gao, D. Craig, V. Vogel and K. Schulten, *Journal of Molecular Biology*, 2002, 323, 939.
- 16 S. Harrison, *Nat Struct Mol Biol*, 2008, 15, 690.
- 17 J. Kovacs, J. Nkolola, H. Peng, A. Cheung, J. Perry, J., C. Miller, M. Seaman, D. Barouch and B. Chen, *Proceedings of the National Academy of Sciences*, 2012, 109, 12111.
- 18 L. Donlon, D. Nordin and D. Frankel, *Soft Matter*, 2012, 8, 9933.
- 19 L. Donlon, A. Penaherrera and D. Frankel, *Soft Matter*, 2013, 9, 2803.
- 20 S. Allen, J. Davies, A. Dawkes, M. Davies, J. Edwards, M. Parker, C. Roberts, J. Sefton, S. Tendler and P. Williams, *FEBS Letters*, 1996, 39, 161.
- 21 P. Williams, A. Moore, M. Stevens, S. Allen, M. Davies, C. Roberts and S. Tendler, *Journal of the Chemical Society, Perkin Transactions* 2000, 2, 5.
- 22 M. Hussain, A. Agnihotri and C. Siedlecki, *Langmuir*, 2005, 21, 6979.
- 23 E. Gee, D. Ingber and C. Stultz, *Plos one*, 2008, 3, e2373.
- 24 A. Oberhauser, C. Badilla-Fernandez, M. Carrion-Vazquez and J. Fernandez, *Journal of Molecular Biology*, 2002, 319, 433.

- 25 D. Craig, A. Krammer, K. Schulten and V. Vogel, *Proceedings of the National Academy of Sciences*, 2001, 98, 5590.
- 26 R. Best, S. Fowler, J. Toca Herrera, A. Steward, E. Paci, and J. Clarke, *Journal of Molecular Biology*, 2003, 330, 867.
- 27 J. Hutter and J. Beschhoefer, *Review of Scientific Instruments*, 1993, 64, 1868.